Distribution Agreement

In presenting this thesis as a partial fulfillment of the requirements for a degree from Emory University, I hereby grant to Emory University and its agents the non-exclusive license to archive, make accessible, and display my thesis in whole or in part in all forms of media, now or hereafter now, including display on the World Wide Web. I understand that I may select some access restrictions as part of the online submission of this thesis. I retain all ownership rights to the copyright of the thesis. I also retain the right to use in future works (such as articles or books) all or part of this thesis.

Yujia Li December 6, 2022

Dopamine modulation of NMDA receptor subunit GluN2A function in indirect pathway striatal projection neurons in Parkinson's Disease

by

Yujia Li

Dr. Stella Papa

Adviser

Biology

Dr. Stella Papa

Adviser

Dr. Dieter Jaeger

Committee Member

Dr. Ellen Hess

Committee Member

2022

Dopamine modulation of NMDA receptor subunit GluN2A function in indirect pathway striatal projection neurons in Parkinson's Disease

By

Yujia Li

Dr. Stella Papa
Adviser

An abstract of
a thesis submitted to the Faculty of Emory College of Arts and Sciences
of Emory University in partial fulfillment
of the requirements of the degree of
Bachelor of Science with Honors

Biology

2022

Abstract

Dopamine modulation of NMDA receptor subunit GluN2A function in indirect pathway striatal projection neurons in Parkinson's Disease

By Yujia Li

Parkinson's disease (PD) is a progressive neurodegenerative disease characterized by the death of dopaminergic neurons in the substantia nigra pars compacta (SNc). Dopaminergic neurons in SNc project to the striatum, the recipient area for information that reach the basal ganglia. Dopamine (DA) modulates striatal projection neurons (SPNs) of the striatum by upregulating the firing rates of SPNs expressing the dopamine 1 receptors (D1Rs) and downregulating the firing rates of SPNs expressing the dopamine 2 receptors (D2Rs). Based on the differential neuronal projections, the two SPN subtypes are known as the direct pathway SPNs (dSPNs) and the indirect pathway SPNs (iSPNs) respectively. Previous studies have found that in PD, the loss of DA modulation may lead to SPN hyperactivity and a differential change in firing patterns between dSPNs and iSPNs. Further evidence suggested that glutamatergic signaling, including NMDA receptor-mediated excitatory postsynaptic currents (EPSCs), may play a role in the altered SPN activities. This study investigated the functional change of the GluN2A subunit of the NMDA receptor (NMDAR) in iSPNs in PD, using a 6-OHDA lesioned hemiparkinsonian rat model. We did not find a significant difference in GluN2A-mediated EPSCs between iSPNs of DA-intact and DA-depleted striatum. iSPN hyperactivity and firing pattern changes in PD are likely not due to changes in Glu2A-mediated EPSC.

Dopamine modulation of NMDA receptor subunit GluN2A function in indirect pathway striatal projection neurons in Parkinson's Disease

By

Yujia Li

Dr. Stella Papa
Adviser

A thesis submitted to the Faculty of Emory College of Arts and Sciences
of Emory University in partial fulfillment
of the requirements of the degree of
Bachelor of Science with Honors

Biology

2022

Acknowledgements

First of all, I would like to thank Dr. Stella Papa for giving me the opportunity to work at her lab and for allowing me to pursue this research topic in a compressed timeline, when the COVID-19 pandemic deterred me from working at the lab for a year. I would also like to thank Dr. Christopher Sinon for performing the electrophysiology experiments and for the consistent amount of time and effort to guide me through every step of this project from data analysis to presentations and to writing of the thesis. I am grateful to my two committee members Dr. Dieter Jaeger and Dr. Ellen Hess for their advice on experimental methods and defining the scope of this project. Lastly, this thesis would have not been made possible without comments for revision from all three of my committee members Dr. Dieter Jaeger, Dr. Ellen Hess and Dr. Stella Papa.

Table of Contents

Introduction

Parkinson's disease is a motor disorder characterized by the degeneration of dopaminergic neurons in the substantia nigra pars compacta (SNc). The dopaminergic neurons in the SNc project to the striatum, a major recipient area for information that reach the basal ganglia neural circuit (Surmeier et al. 2014). The striatum also receives glutamatergic innervations from the cortex and the thalamus (Wall et al. 2013).

Striatal projections neurons (SPNs), the major neuron cell type in the striatum, are GABAergic. They exhibit two subtypes differentially regulated by dopamine (DA). SPNs expressing the dopamine 1 receptor (D1R) undergo increased intrinsic excitability upon DA binding, while those expressing the dopamine 2 receptor (D2R) undergo decreased intrinsic excitability. Increased firing rates of D1R-expressing SPNs inhibits subsequent GABAergic neurons in the globus pallidus internal (GPi) and the substantia nigra reticulata (SNr), which reduces thalamic inhibition and promotes movement. Decreased firing rates of D2R-expressing SPNs disinhibits neurons in the globus pallidus external (GPe) and reduces excitatory drives from the subthalamic nucleus (STN) to GPi and SNr, which also reduces thalamic inhibition and promotes movement (Freeze et al. 2013). Thus, dopamine promotes movement through the direct and indirect pathway. D1R-expressing SPNs project to the direct pathway neurons, while D2R-expressing SPNs project to the indirect pathway neurons. The two SPN subtypes are also known as direct pathway SPNs (dSPNs) and indirect pathway SPNs (iSPNs) respectively (Surmeier et al. 2014).

In Parkinson's disease, the rate model predicts that after the loss of DA modulation, dSPNs undergo decreased firing activities and iSPNs undergo increased firing activities. Firing rate changes in both SPN subtypes result in decreased GPi/SNr neuron inhibition and a larger

degree of thalamic inhibition. The alterations in firing rates could account for hypokinetic disorders such as Parkinson's disease (Delong 1990). However, in MPTP-treated severe Parkinsonian primates, both iSPNs and dSPNs showed hyperactivities with firing rates 20-30 times higher than the normal spontaneous firing rates at 0.5-2 Hz (Liang et al. 2008). Furthermore, iSPNs exhibited a pausing activity pattern, while dSPNs exhibited a bursty firing pattern, suggesting differential regulation of the two SPN subtypes after DA loss (Singh et al. 2015). These evidence called into question the rate model that only accounted for the alterations in dopamine modulation on SPNs but not in other neurotransmitters in PD.

Glutamate signaling has been shown to play a role in SPN activities after the loss of striatal DA modulation. N-methyl-D-aspartate (NMDA) receptor or α-amino-3-hydroxy-5-methyl-4-isoxazolepropionic acid (AMPA) receptor antagonists reduced SPN hyperactivity in MPTP-treated severe Parkinsonian primates (Singh et al. 2018). At the corticostriatal synapse, the amplitudes of evoked NMDA receptor-mediated EPSCs (NMDAR-EPSCs) of iSPNs in DA-depleted striatum was larger compared to iSPNs from normal striatum, but no such difference was found in dSPNs (Fieblinger 2014). The differential change in glutamatergic currents in the PD-state dSPNs and iSPNs led us to hypothesize that alterations in NMDAR-mediated EPSCs could underlie the mechanism of SPN hyperactivity in Parkinson's disease. In this study, we explored the evoked NMDAR-EPSCs mediated by the GluN2A subunit in iSPNs from normal and DA-depleted striatum, using the 6-hydroxydopamine hydrochloride (6-OHDA) lesioned hemiparkinsonian rats. We hope to investigate whether the change in the GluN2A function underlie the mechanism of SPN hyperactivity in PD.

The NMDA receptor is a voltage-gated cation channel that requires coactivation by glycine and glutamate. It is a heterotetrametric complex consisted of two GluN1 subunits and

two GluN2 (GluN2A-GluN2D) subunits or one GluN2 subunit and one GluN3 (GluN3A or GluN3B) subunit (Traynelis et al, 2010). GluN2B-mediated NMDAR-EPSCs have been shown to decrease in PD-state SPNs, and the GluN2D-mediated NMDAR-EPSCs, not present in normal SPNs, have been shown to emerge in SPNs after the loss of DA modulation (Zhang et al. 2015). Alterations in GluN2A subunit function have not been explored in specific SPN subtypes.

In this study, we set out to investigate the GluN2A-mediated NMDAR-EPSCs in response to glutamate in iSPNs from DA-intact and DA-depleted striata. rAAV8-D2SP-eYFP virus was injected bilaterally in the striata of 6-OHDA lesioned hemiparkinsonian rats to introduce fluorescence into iSPNs. The virus specificity for iSPNs was confirmed using RNAscope. Our results did not show a significant change in GluN2A function after the loss of DA modulation, indicating that iSPN hyperactivity and altered firing patterns in PD could more likely be explained by altered NMDAR-EPSCs mediated by the GluN2B and/or GluN2D subunits.

Materials and Methods

Ethics Statement

All procedures were approved by the Emory University *Institutional Animal Care and Use Committee* and were performed in accordance with the National Institutes of Health *Guide for the Care and Use of Laboratory Animals*.

6-OHDA lesioned hemiparkinsonian rat model

8-week-old Sprague Dawley rats (n=13) were anesthetized with isoflurane (1.5%-2.5% in O_2) in a sealed container. The rats were positioned on a stereotaxic frame with the incisor teeth

fixed, the noses in the nose cone, and the horizontal ear bar aligned with the interaural line. A 15 mm incision was made on the head skin to expose the skull. 6-OHDA injections were made to aim for the medial forebrain bundle at stereotaxic coordinates 4.0 mm anterior and 1.3 mm lateral to the midpoint of the interaural line, and at a depth 8.4 mm relative to the skull surface. A total of 12 μg 6-OHDA was dissolved 2μg/μl in 0.02% ascorbic acid. A micropump was used to deliver the 6-OHDA solution at a rate of 1 μl/min. The microsyringe needle was left in the injection site for 5 min before it was slowly withdrawn at 1 mm/min. All 6-OHDA injections were made unilaterally on the left hemisphere.

Virus injection

Virus injections of rAAV8-D2SP-eYFP were made in the dorsal lateral striatum (stereotaxic coordinates 8.4 mm anterior to the interaural line, 4.1 mm lateral to the midline and at depths -6.2 mm and -5.2 mm ventral to the skull surface with 1.5 μl and 0.5 μl virus solution respectively) of rats (n=15). Virus solution (1-2.0E+12 vg/ml) was loaded in a Hamilton syringe and injected at 0.5 μl /min. 2 wild type rats received unilateral injections of rAAV8-D2SP-eYFP. 13 rats received bilateral injections of rAAV8-D2SP-eYFP at the same time of 6-OHDA lesion surgery.

Apomorphine Test

3 weeks after the 6-OHDA lesion surgery, apomorphine (0.05 mg/kg, s.c.) was administered to screen for the extent of dopaminergic cell death in SNc. Rats were placed in a jacket connected to a rotameter. Animals performing more than 100 full contralateral rotations in 1 h were considered to have a full lesion with >95% dopaminergic cell death in SNc. Those

performed 50-100 or 0-50 rotations were considered to have a partial lesion or no lesion with 90-95% and <90% SNc dopaminergic cell loss correspondingly (Papa 1994). We recorded in iSPNs from the lesioned hemispheres of all rats with a full lesion (n=6) and one rat that performed 80 rotations. For control iSPNs, we recorded from the intact hemispheres of rats with full, partial or no lesion (n=5).

Brain Slice Preparation

6-OHDA lesioned rats were deeply anesthetized and decapitated. The brain was dissected under immersion in a cold modified artificial cerebrospinal fluid (ACSF) solution with the composition (in mM): 93 Choline chloride, 2.5 KCl, 1.2 NaH_2PO_4, 2.4 $CaCl_2$, 25 glucose and 30 $NaHCO_3$, 2 Thiourea, 5 Na-ascorbate, 20 HEPES, 3 Na-pyruvate, 12 N-acetyl-L-cysteine, 10 $MgSO_4$ and 0.5 $CaCl_2$ constantly supplied with 95% O_2 – 5% CO_2 gas mixture. 260-300 μm coronal brain slices were cut using a vibratome at room temperature in the previously mentioned cold modified ACSF. Brain slices were recovered for at least 1 h in the HEPES-ACSF recovery solution (92 mM NaCl, 2.5 mM KCl, 1.2 mM NaH_2PO_4, 25 mM glucose and 30 mM $NaHCO_3$, 2 mM Thiourea, 5 mM Na-ascorbate, 20 mM HEPES, 3 mM Na-pyruvate, 12 mM N-acetyl-L-cysteine, 2 mM $MgSO_4$ and 2 mM $CaCl_2$ with 95% O_2 – 5% CO_2 continuous gas mixture) at room temperature. Then, the brain slices were transferred to a recording chamber with the Krebs solution (124 mM NaCl, 3 mM KCl, 1 mM NaH_2PO_4, 26 mM $NaHCO_3$, 13.89 mM glucose, 1.2 mM $MgSO_4$ and 2.4 mM $CaCl_2$ with 95% O_2 – 5% CO_2 continuous oxygenation) at 37 °C for 10-12 mins. Electrophysiology recordings were made from 1-9 h post sacrifice.

Whole Cell Electrophysiology Recording

Whole cell voltage-clamp recordings were made with borosilicate glass electrodes WPI TW150F-4 (1.5 mm OD, 1.12 mm ID, length 4 inch). The pipette resistance ranged from 4.5-6.5 MΩ. Electrodes were filled with internal solution with the composition (in mM) 120 CH_3O_3SCs, 15 CsCl, 8 NaCl, 0.2 EGTA, 10 HEPES acid, 2 Mg_2ATP, 0.3 NaGTP, 10 TEA, 5 QX-314, 2.7 biocytin. iSPNs were identified under a fluorescence microscopy, and whole cell voltage-clamp recordings were performed in fluorescent SPNs from the dorsal lateral striatum. The recordings were made with a Multiclamp 700B amplifier.

A bipolar concentric stimulating electrode was placed at the corpus collosum to evoke glutamatergic EPSCs every 30 seconds. Cells were successfully patched when a tight seal above 1 GΩ formed. We then break through the cell membrane to record from the cytosol. iSPNs were voltage-clamped to +40 mV. Membrane currents and access resistance were monitored throughout the experiment.

All recordings were made in the Krebs recording solution described above with constant oxygenation (95% O_2 – 5% CO_2) at 32 °C. First, the GABA receptor antagonist picrotoxin (50 μM) and the AMPA receptor antagonist NBQX (10 μM) were washed in for 5-10 mins, and evoked NMDAR-EPSCs were recorded for 5 min. Then, GluN2A-specific inhibitor MPX-004 (5-(((3-chloro-4-fluorophenyl) sulfonamido) methyl)-N-((2-methylthiazol-5-yl) methyl) pyrazine-2-carboxamide) (10 μM, Volkmann et al. 2016) was introduced for 5 mins before recording evoked NMDAR-EPSCs for 5 min. Lastly, the NMDAR antagonist APV (100 μM) was washed in for 2 min before the evoked EPSCs were recorded for 2 min (Fig. 4).

At the end of each EPSC trace, 3 capacitive currents were produced by changing the holding voltage by 5mV above and below +40mV in an alternating pattern. The capacitive

currents and membrane resistances were calculated and averaged among the 3 stimulations. A stable membrane resistance throughout the recording indicates good seal quality throughout the recording period. 4 cells (1 from the intact group and 3 from the 6-OHDA lesioned group) were excluded because of the significant changes in membrane resistance above 20% after the MPX-004 wash-in.

RNAscope Assay

After the striatal injections of the virus rAAV8-D2SP-eYFP, 2 wild type rats were anesthetized with isoflurane and decapitated. Brains were harvested and snap-frozen in isopentane cooled on dry ice for 30 s-1 min before storing in an airtight container at -80 °C. Fresh frozen brain tissues were equilibrated to -20 °C in a cryostat for 1 h, then 15 μm coronal sections were cut and mounted on precleaned Superfrost Plus® slides. The brain sections were stored in an airtight container at -80 °C.

RNAscope Multiplex Fluorescent Reagent Kit v2 Assay (ACD) was performed following standard procedures. Probes EYFP-C1, Rn-Drd2-C2 and Rn-Drd1-C3 were used to target eYFP, D2R and D1R mRNA. The probes were labeled with Opal 520, Opal 570 and Opal 650 dyes (respectively) diluted with TSA buffer at 1:1000.

Fresh frozen brain sections were fixed in 4% PFA for 15 min at 4 °C and were dehydrated in 50%, 70% and 100% EtOH series for 5 min each at room temperature (RT). Glass slides were held in place by EZ-Batch Slide Holder (ACD) and were placed in the HybEZ Humidity Control Tray (ACD) above a wet humidifying paper. All incubation steps took place in the HybEZ Humidity Control Tray. The brain sections were treated with hydrogen peroxide for 10 min at RT and Protease IV for 30 min at RT with ddH_2O and 1x PBS double wash steps after

the incubation period with each reagent respectively. All incubation steps were done in the HybEZ II Oven (ACD) at 40 °C. First, the probe mix was hybridized at 40 °C for 2 h. Then, amplification probes 1 and 2 (AMP 1 and AMP 2) were applied for 30 min and amplification probe 3 (AMP 3) for 15 min at 40 °C in sequence. Finally, horseradish peroxidase C1 (HRP-C1) was incubated for 20 min. Opal 520 dye was incubated for 30 min and HRP blocker for 15 min at 40 °C. The same sequence was applied for HRP-C2 and HRP-C3 with Opal 570 and Opal 620 fluorescent dyes correspondingly. DAPI was applied for 30 s at RT. Eventually, the Prolong Gold Antifade Mountant was applied at RT and then #1.5 coverslips were placed over brain sections. Brain slides were dried overnight at RT and stored at 4 °C in the dark. The brain sections were imaged on a confocal microscope (Leica SP 8) under the 20x and 40x objectives with excitation lasers at wavelengths 488 nm for the Opal 520 dye, 561 nm for the Opal 570 dye and 623 nm for the Opal 650 dye.

Statistical Analysis

Chi-squared test was used to quantify the difference between the occurrences of eYFP positive SPN colocalization with D2R and the half of total number of cells, indicating colocalization by chance.

Evoked EPSC traces were processed using a lowpass 8 pole Bessel filter with -3dB cutoff at 2000 Hz and were averaged in Clampfit. Baseline recording traces were averaged from at least 9 traces, excluding occasional traces with artifacts. Traces recorded with MPX-004 were averaged among the last 10 traces, and traces recorded with APV were averaged among the last 4 traces. All filtered and averaged traces were fitted to a double exponential decay model in

ChannelLab to at least 0.7 goodness of fit. Decay model parameters such as start time, peak scan, number of fit points and parse fit points were kept consistent for all traces from the same cell.

Mann-Whitney U test was performed for evoked EPSC amplitudes normalized to the baseline recording EPSC amplitudes to test whether the difference between intact and 6-OHDA-lesioned iSPNs is significant at each trace number. Mann-Whitney U test was also performed on normalized NMDAR-EPSC amplitudes of averaged traces from MPX-004 recordings between intact and 6-OHDA lesioned cells. Paired t-test was used to compare the average amplitude differences between NMDAR-EPSC amplitudes of baseline recordings and recordings with MPX-004 and between recordings with MPX-004 and recordings with APV. Paired t-test was also used to compare the weighted tau of averaged traces between baseline recordings and recordings with MPX-004.

Results

rAAV8-D2SP-eYFP is 89% specific for iSPNs

Figure 2 shows that 89.4% of rAAV8-D2SP-eYFP infected cells expressing eYFP colocalized with D2R, an iSPN marker. 10.6% of the infected neurons expressing eYFP colocalized with D1R, a dSPN marker. No virus positive neurons colocalized with both D1R and D2R. Chi-squared test showed that occurrences of colocalization between eYFP and D2R is significantly higher than colocalization by chance at $p<0.001$. rAAV8-D2SP-eYFP is at least 89% specific for iSPNs.

Evoked GluN2A-mediated NMDAR-EPSC amplitudes did not significantly differ between iSPNs of the intact hemispheres and DA-depleted hemispheres.

During the apomorphine test, 6 rats performed more than 100 full contralateral rotations in 1 h, and were considered to have full 6-OHDA lesions. 7 rats performed <100 full contralateral rotations in 1 h, and they were considered to have partial or no lesions (Fig. 3).

Figure 5 showed that evoked NMDAR-EPSC amplitudes are stable during baseline recordings from trace 1-10. After applying MPX-004, NMDAR-EPSC amplitudes decreased gradually from trace 11-20 and stabilized at ~75% through trace 21-30. For recordings in the presence of APV, eEPSC amplitudes gradually decreased from trace 31-34 and stabilized at ~0% through traces 34-38, demonstrating that all observed currents were mediated by NMDARs (Fig. 5). No significant difference in evoked NMDAR-EPSC amplitudes was found between iSPNs from the intact and 6-OHDA lesioned hemispheres in all traces throughout the recording period.

For iSPNs from the intact hemispheres, MPX-004 reduced the evoked NMDAR-EPSC amplitudes by 25.84% from baseline ($p<0.001$), and for iSPNs in the 6-OHDA-lesioned hemispheres, MPX-004 reduced the evoked NMDAR-EPSC amplitudes by 34.75% ($p<0.01$). NMDAR composed of the GluN2A subunit contributes to ~25% of total NMDAR-EPSCs in normal state iSPNs and it contributes to ~35% of total NMDAR-EPSC in iSPNs in 6-OHDA lesioned group iSPNs. APV exerted an inhibitory effect that significantly decreased evoked NMDAR-EPSC amplitudes to about 0% for all iSPNs recorded ($p<0.001$ intact and 6-OHDA lesioned, Fig. 6).

After GluN2A subunit inhibition, evoked NMDAR-EPSC amplitudes did not show a significant difference, although a greater decrease in amplitudes was observed in PD-state iSPNs (Fig. 7). The extent of DA depletion and GluN2A-inhibited NMDAR-EPSC amplitudes of iSPNs in DA-depleted striatum showed a nonsignificant negative correlation at $r^2 = 0.371$ (Fig. 8). Two iSPNs from the rat with 80 contralateral rotations exhibited similar evoked NMDAR-EPSC

amplitudes to iSPNs from rats with >100 rotations. This could mean that the rat that performed 80 rotations might have obtained a similar lesion extent to the lesions in full-lesioned animals. Figure 8 also showed three 6-OHDA lesioned group iSPNs with lower NMDAR-EPSC amplitudes than the rest. These outliers are likely not due to the inclusion of the partial-lesioned animal with 80 contralateral rotations (Fig. 8).

Lastly, NMDAR deactivation time, quantified by weighted tau, increased significantly for both normal and 6-OHDA-lesioned group iSPNs after GluN2A inhibition (intact $p<0.01$, 6-OHDA lesioned $p<0.05$). Because NMDARs composed of the GluN2A subunit exhibit shorter deactivation time than those composed of the GluN2B subunit, the significant increase in NMDAR deactivation time after GluN2A inhibition indirectly confirms MPX-004's inhibitory effect on the GluN2A subunit. The percent increase in deactivation time was not significantly different between the intact and 6-OHDA lesioned group iSPNs ($p=0.91$ n.s., Fig. 9).

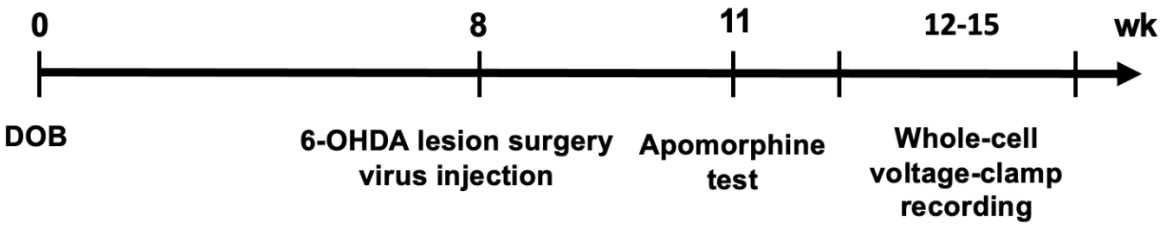

Figure 1. Animal manipulation timeline for the whole-cell voltage clamp electrophysiology experiment.

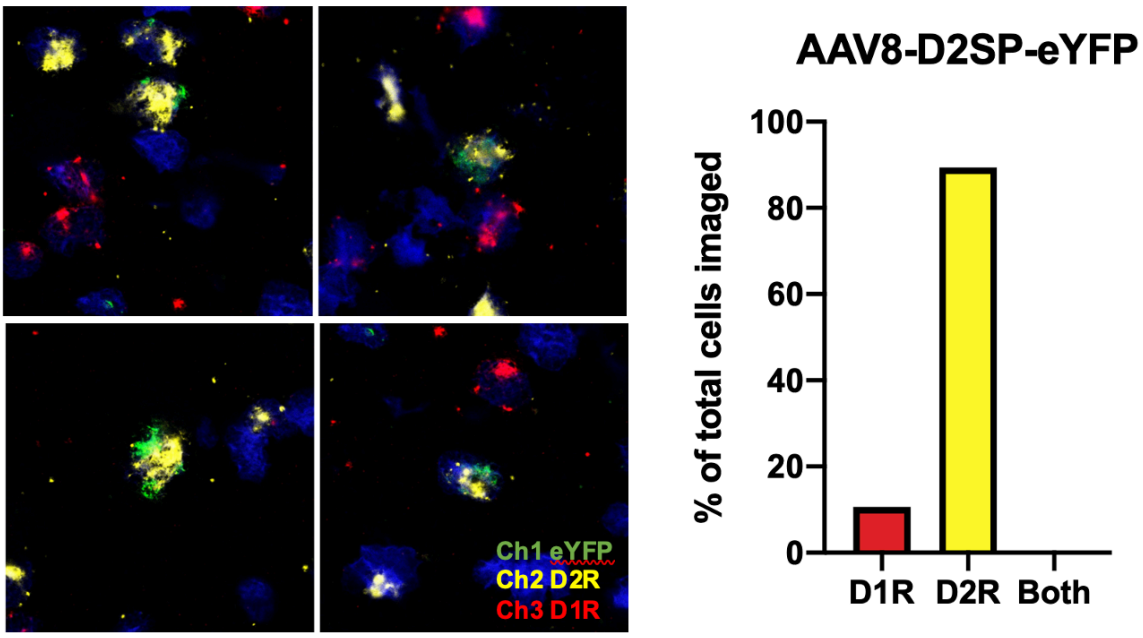

Figure 2. rAAV8-D2SP-eYFP virus specificity tested by (A) fluorescently staining eYFP (green), D2R (yellow) and D1R (red) mRNA using RNAscope. (B) 89.6 % eYFP-positive cells colocalized with D2R (rats n=2, 42 out of 47 cells), 10.6% eYFP-positive cells colocalized with D1R (5 cells out of 47 cells) and no eYFP-positive cells colocalized with both D1R and D2R (0 cells out of 47 cells). eYFP-positive cell colocalization with D2R is significantly higher than random colocalization (23.5 cells out of 47 cells). ***$p<0.001$.

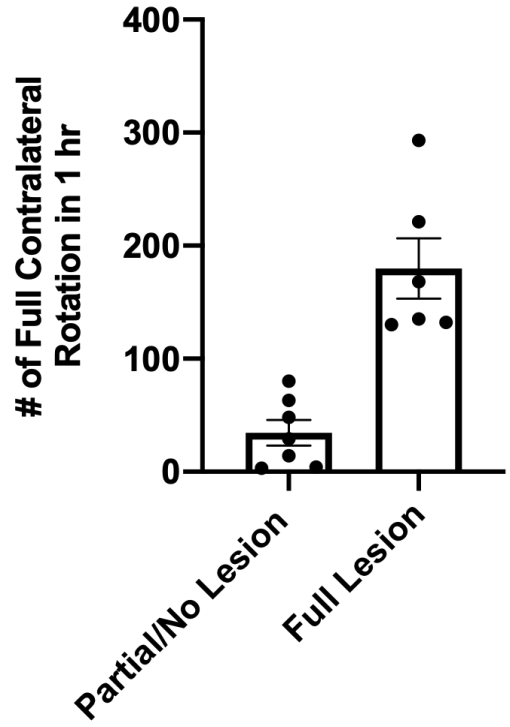

Figure 3. Apomorphine test screened 6-OHDA-lesioned rats for the extent of dopaminergic cell death in SNc. 6 rats performed 100 or more full contralateral rotations in 1 h, indicating a full lesion. 7 rats performed <100 full contralateral rotations in 1 h, which indicates partial or no lesion.

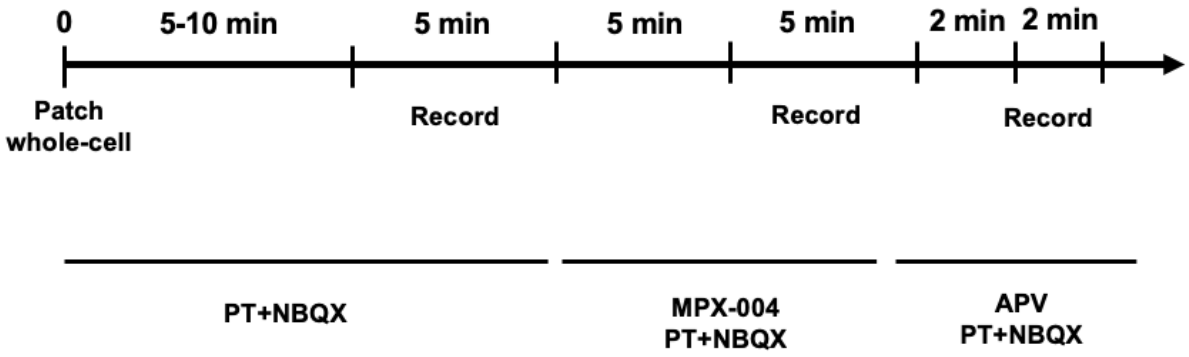

Figure 4. Whole cell voltage-clamp recording experiment timeline.

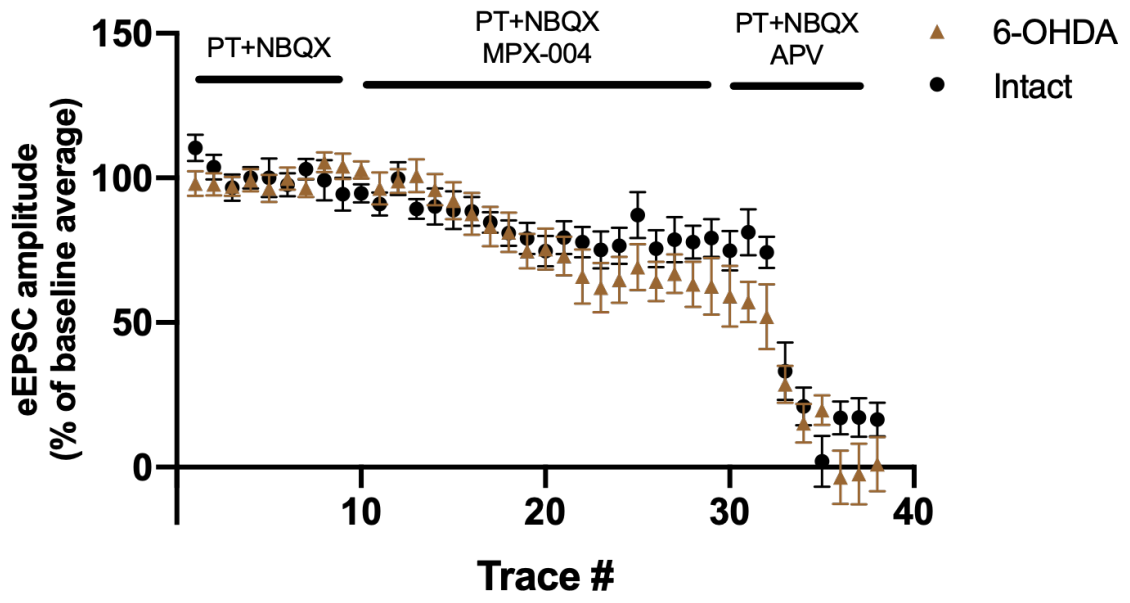

Figure 5. Time course of the MPX-004 (10 uM) and APV (100 uM) drug effect on the eEPSC amplitudes expressed as % of baseline (mean ± S.E.M) in iSPNs of intact (n=12) and DA-depleted striatum (n=10). P>0.05 n.s. for all traces.

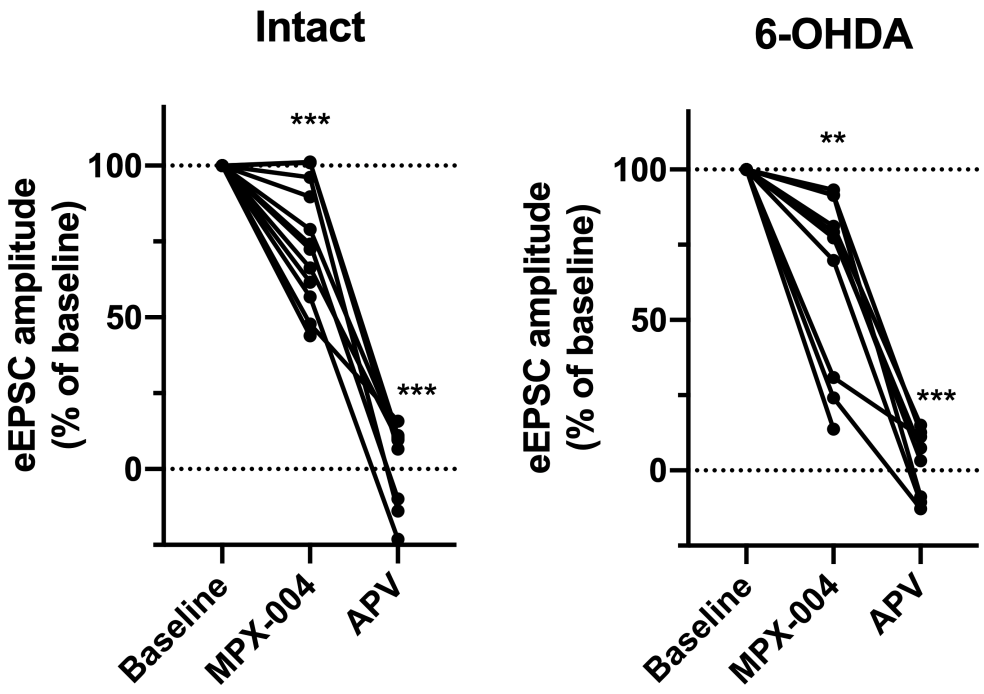

Figure 6. Drug effects of MPX-004 and APV on evoked NMDAR-EPSC amplitude, expressed as % of baseline, in iSPNs from intact (n=12 cells) or DA-depleted (n=10 cells) striatum. Evoked NMDAR-EPSC amplitudes decreased significantly from baseline to recordings with MPX-004 in both intact ($p<0.001$***) and 6-OHDA lesioned ($p<0.01$**) group iSPNs. eEPSC amplitudes decreased from MPX-004 recordings to APV recordings in both intact ($p<0.001$***) and 6-OHDA lesioned ($p<0.001$***) iSPNs. MPX-004 inhibits about 25% NMDAR-EPSCs that are likely mediated by NMDARs composed of the GluN2A subunit. APV inhibits almost all NMDAR currents, indicating that all observed currents are mediated by NMDARs.

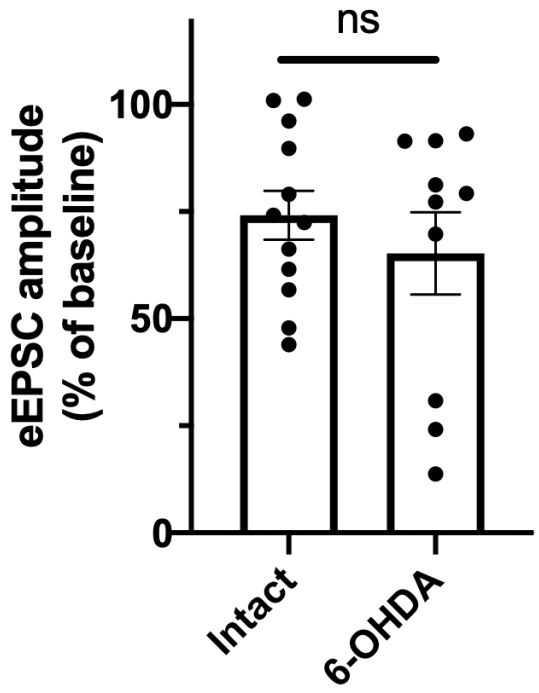

Figure 7. Average effect of MPX-004 on evoked NMDAR-EPSC amplitudes in iSPNs from intact (n=12) and DA-depleted striatum (n=10). P=0.437 n.s.

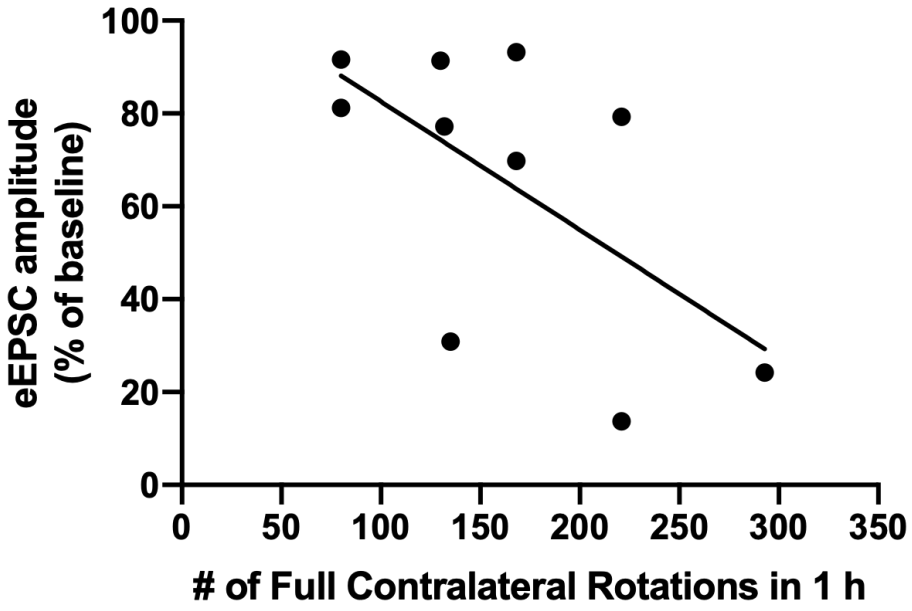

Figure 8. The number of full contralateral rotations performed during the apomorphine test and the evoked NMDAR-EPSC amplitudes of 6-OHDA lesioned hemisphere iSPNs recorded after GluN2A inhibition showed a nonsignificant negative correlation. P=0.061, n.s. $r^2 = 0.371$

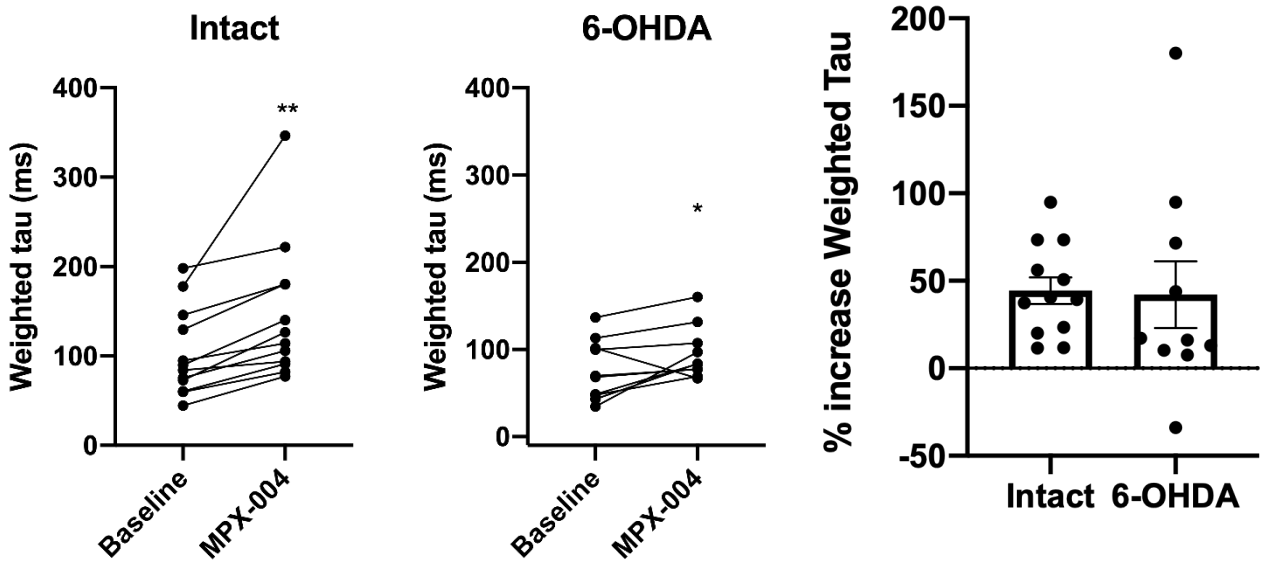

Figure 9. MPX-004 effects on average NMDAR deactivation time, measured by weighted tau. A) Both intact ($p<0.01$**) and 6-OHDA lesioned ($p<0.05$*) iSPNs show an increased NMDAR deactivation time after GluN2A inhibition. B) % increase in deactivation time did not significantly differ between intact and 6-OHDA lesioned group iSPN. $p=0.91$ n.s.

Discussion

A previous study showed that the virus construct rAAV8-D2SP-eYFP was 98.2% specific for iSPNs in the Nucleus accumbens (NAc) among 218 neurons in 2 rats. The same study also demonstrated that cells infected by D2SP-eChR2-eYFP, a viral construct with the same D2R-specific promoter (D2SP) as rAAV8-D2SP-eYFP, had minimal colocalization with cholinergic interneurons in NAc. Out of the 782 virus-positive cells and 93 cholinergic interneurons from brain slices of 6 rats, only 3 virus-positive cells colocalized with cholinergic interneurons (Zalocusky et al. 2016). We are confident that at least 89% of the fluorescent cells recorded in our whole-cell voltage-clamp electrophysiology experiments are iSPNs.

Although no statistically significant difference was found between GluN2A-mediated EPSCs of normal and PD-state iSPNs, 3 out of 10 iSPNs in the 6-OHDA lesioned group presented greater GluN2A-mediated EPSC (Fig. 7), which led us to question whether a real increase in GluN2A function is present in iSPNs after the loss of DA control. Figure 8 showed that 2 out of the 3 outliers came from rats with high rotation numbers above 200. However, in the apomorphine test, because all full-lesioned rats should have >95% dopaminergic cell loss in the SNc, the extent of the 6-OHDA lesion in rats exhibiting 100 rotations should not too much different from those that performed >200 rotations (Papa 1994). We believe that the 3 outliers are possibly due to chance, and in a small sample size of 10 cells, they seem to hold a greater weight than they would in a large sample size. Repeating the current experiment in more iSPNs from the 6-OHDA lesioned hemisphere could help decrease the weight of outliers and help confirm the nonsignificant change in GluN2A subunit function.

Evidence of synaptic GluN2A expression could support our nonsignificant finding. Paillé et al. (2010) compared the postsynaptic membrane expression of the GluN2A subunit in SPNs

among sham, partial and full 6-OHDA lesioned rats. The full-lesioned rats had nonsignificantly higher expression than sham-lesioned animals. Although post-synaptic membrane expression does not guarantee synaptic function, the nonsignificantly increased GluN2A expression of PD-state SPNs aligns with our result that showed nonsignificantly higher GluN2A-mediated EPSCs of PD-state iSPNs. Future experiments could quantify GluN2A expression in iSPNs to further support nonsignificant change in GluN2A function in PD.

Alterations in GluN2B and GluN2D subunit functions could underlie SPN hyperactivities and altered firing patterns in PD. GluN2B-mediated EPSCs is significantly decreased in PD-state SPNs (Zhang et al. 2015). Postsynaptic membrane expression of GluN2B decreased in MPTP-treated mild and severe Parkinsonian nonhuman primates (Mellone et al. 2015). An immunohistochemistry experiment showed that GluN2D subunit was expressed in SPNs from the lesioned hemisphere of full 6-OHDA lesioned animals, but control SPNs in the intact hemispheres showed no GluN2D expression (Mellone et al. 2019). This algins with the emergence of GluN2D-mediated EPSCs in the PD-state SPNs of 6-OHDA lesioned mice (Zhang et al. 2015). Future experiments could explore whether alterations in GluN2B and GluN2D function occurs in both iSPNs and dSPNs.

A limitation of this study is that control iSPNs were recorded from the intact hemispheres of 6-OHDA lesioned animals, not from sham-lesioned animals. Alterations in the intact hemisphere to compensate for motor deficits caused by the 6-OHDA lesion remain unknown. Furthermore, because the 6-OHDA lesioned rat model is an acute model of PD, it does not reflect the progression of the disease in patients. GluN2A dysfunction in SPNs could still occur due to factors other than the loss of DA modulation. For example, alpha-synuclein, an extracellular protein that aggregates gradually to form insoluble Lewy bodies, decreased

GluN2A-mediated EPSCs and postsynaptic membrane expression of GluN2A in SPNs (Durante et al. 2019).

Characterization of changes in GluN2 subunit function in iSPNs and dSPNs separately could further explain the differential firing patterns observed. In addition, current PD treatment focuses on dopamine replacement through oral ingestion the DA precursor, Levodopa. Patients under long term Levodopa treatment develop involuntary movements, known as Levodopa-induced dyskinesia. GluN2 subunits could be a pharmacological target for drugs that restore SPN activities and alleviate the motor symptoms of PD. Characterization of GluN2 changes in SPN subtypes could help develop drugs targeting specific motor pathways without concerns for off-target effects.

Conclusion

In this study, we found a nonsignificant difference between GluN2A-mediated NMDAR-EPSC amplitudes of iSPNs in dopamine-intact and dopamine-depleted striatum using the 6-OHDA lesioned hemiparkinsonian rat model. Changes in glutamatergic signaling may underlie SPN hyperactivity and the differential alterations of firing patterns in dSPNs and iSPNs in PD, but in this study that only investigated functional changes in one GluN2 subunit in one SPN subtype, we did not find support for the mechanism of altered SPN activities through GluN2A-mediated EPSCs in Parkinson's Disease.

References

DeLong, M. R., 1990 Primate models of movement disorders of basal ganglia origin. Trends Neurosci 13**:** 281-285.

Durante, V., A. de Iure, V. Loffredo, N. Vaikath, M. De Risi *et al.*, 2019 Alpha-synuclein targets GluN2A NMDA receptor subunit causing striatal synaptic dysfunction and visuospatial memory alteration. Brain 142**:** 1365-1385.

Fieblinger, T., S. M. Graves, L. E. Sebel, C. Alcacer, J. L. Plotkin *et al.*, 2014 Cell type-specific plasticity of striatal projection neurons in parkinsonism and L-DOPA-induced dyskinesia. Nat Commun 5**:** 5316.

Freeze, B. S., A. V. Kravitz, N. Hammack, J. D. Berke and A. C. Kreitzer, 2013 Control of basal ganglia output by direct and indirect pathway projection neurons. J Neurosci 33**:** 18531-18539.

Liang, L., M. R. DeLong and S. M. Papa, 2008 Inversion of dopamine responses in striatal medium spiny neurons and involuntary movements. J Neurosci 28**:** 7537-7547.

Mellone, M., J. Stanic, L. F. Hernandez, E. Iglesias, E. Zianni *et al.*, 2015 NMDA receptor GluN2A/GluN2B subunit ratio as synaptic trait of levodopa-induced dyskinesias: from experimental models to patients. Frontiers in cellular neuroscience 9**:** 245-245.

Mellone, M., E. Zianni, J. Stanic, F. Campanelli, G. Marino et al., 2019 NMDA receptor GluN2D subunit participates to levodopa-induced dyskinesia pathophysiology. Neurobiology of Disease 121: 338-349.

Paillé, V., B. Picconi, V. Bagetta, V. Ghiglieri, C. Sgobio *et al.*, 2010 Distinct levels of dopamine denervation differentially alter striatal synaptic plasticity and NMDA receptor subunit composition. J Neurosci 30**:** 14182-14193.

Papa, S. M., T. M. Engber, A. M. Kask and T. N. Chase, 1994 Motor fluctuations in levodopa treated parkinsonian rats: relation to lesion extent and treatment duration. Brain Res 662**:** 69-74.

Singh, A., M. A. Jenkins, K. J. Burke, Jr., G. Beck, A. Jenkins *et al.*, 2018 Glutamatergic Tuning of Hyperactive Striatal Projection Neurons Controls the Motor Response to Dopamine Replacement in Parkinsonian Primates. Cell reports 22**:** 941-952.

Singh, A., L. Liang, Y. Kaneoke, X. Cao and S. M. Papa, 2015 Dopamine regulates distinctively the activity patterns of striatal output neurons in advanced parkinsonian primates. J Neurophysiol 113**:** 1533-1544.

Surmeier, D. J., S. M. Graves and W. Shen, 2014 Dopaminergic modulation of striatal networks in health and Parkinson's disease. Curr Opin Neurobiol 29**:** 109-117.

Traynelis, S. F., L. P. Wollmuth, C. J. McBain, F. S. Menniti, K. M. Vance *et al.*, 2010 Glutamate receptor ion channels: structure, regulation, and function. Pharmacological reviews 62**:** 405-496.

Volkmann, R. A., C. M. Fanger, D. R. Anderson, V. R. Sirivolu, K. Paschetto *et al.*, 2016 MPX-004 and MPX-007: New Pharmacological Tools to Study the Physiology of NMDA Receptors Containing the GluN2A Subunit. PLoS One 11**:** e0148129.

Wall, N. R., M. De La Parra, E. M. Callaway and A. C. Kreitzer, 2013 Differential innervation of direct- and indirect-pathway striatal projection neurons. Neuron 79**:** 347-360.

Zalocusky, K. A., C. Ramakrishnan, T. N. Lerner, T. J. Davidson, B. Knutson *et al.*, 2016 Nucleus accumbens D2R cells signal prior outcomes and control risky decision-making. Nature 531**:** 642-646.

Zhang, X., and K. Chergui, 2015 Dopamine depletion of the striatum causes a cell-type specific reorganization of GluN2B- and GluN2D-containing NMDA receptors. Neuropharmacology 92**:** 108-115.